Supplementary information for: Geometry, mass balance, and thinning at Eklutna Glacier, Alaska: an altitude–mass–balance feedback with implications for water resources

LOUIS C. SASS, MICHAEL G. LOSO, JASON GECK, EVAN E. THOMS, DANIEL MCGRATH

Correspondence: Louis C. Sass <lsass@usgs.gov>

S1 Additional glacier geometries

In 2007, 2011, 2012, and 2014 we analyzed partial coverage surface elevation datasets (Table S3). The 2007, 2011, and 2012 acquisitions were made with the University of Alaska Fairbanks Glacier LiDAR (Larsen, 2010; Larsen and others, 2015). These data are a series of discrete profiles (2007) or swaths (2011 and 2012). The systems used to collect the data have been described previously (Echelmeyer and others, 1996; Arendt and others, 2002; Johnson and others, 2013). Three profiles were collected on 6 May 2007 (118 days before the fall mass balance measurements that year), including one profile along the centerline of the west branch, and two profiles distributed on either side of the centerline of the main branch. The profiles have 1.5 m horizontal point spacing and a reported 0.3 m vertical accuracy. On 29 August 2011 (20 days prior to the fall mass balance measurements), and again on 22 August 2012 (18 days prior to the fall mass balance measurements), three swaths were collected along the same flight paths as the earlier profiles. The swaths are ~ 500 m wide, have a nominal post spacing of 1 m, and have a reported vertical accuracy of 0.3 m. The point-cloud from the swath data was filtered for outliers and gridded at 2 m. The 2014 surface elevation dataset is from Worldview 2 stereo pairs acquired on 19 August (33 days prior to the fall mass balance measurements). The same photogrammetric methods were used as in the 2015 Worldview3 images.

S2 Glacier surface elevations

This explains the differences in our methods as we dealt with spatially incomplete surface elevation datasets.

S2.1 Co-registration and DEM differencing

For the partial data sets we used the 2010 LiDAR-based DEMas a reference, and differenced each of the other data sets from it. Similar to the complete data sets, we used universal co-registration (Nuth and Kääb, 2011) to make minor datum adjustments to match the 2010 DEM. We differenced the datasets directly on each products native postings (grid cell centers for 2011, 2012, and 2014 gridded datasets; profile coordinates for the 2007 profiles) using a bilinear interpolation of the 2010 DEM. We used available data within each bin (colored areas in Fig. S1) to estimate the elevation change as the

median difference in each bin to avoid biases resulting from advection of crevasses and small scale topography (Johnson and others, 2013; Larsen and others, 2015) in the incomplete datasets.

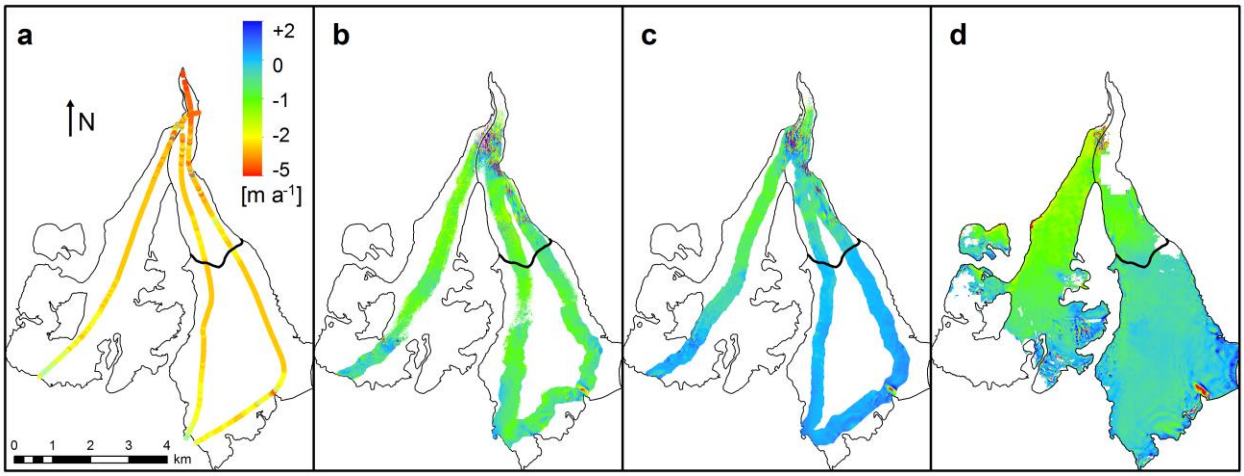

Fig. S1 Raw surface elevation change on Eklutna Glacier for additional measurement intervals between 2007 and 2014: a) 2007–2010, b) 2010–2011, c) 2010–2012, and d) 2010–2014. Colored areas indicate overlapping measurements for each interval, and color bars indicate elevation changes in meters per year. The upper basin of the main branch (>1360 m in 2010) is demarcated by the black line. Each panel has the same extent as figure 1c, and shows the extent of the glacier corresponding to the first year of the interval.

S3 **Uncertainties in the additional data sets**

S3.1. 2007–2010

Both the 2007 LiDAR profiles and the 2010 LiDAR have nominal absolute errors of 0.3 m. For this period we estimate the bias by examining the differences between elevations of stable, off-glacier areas after the DEMs were co-registered. We make the conservative assumption of a high degree of spatial auto-correlation, and use the normalized median absolute deviation (NMAD), a robust statistic appropriate for strongly non-Gaussian populations associated with elevation differences (Höhle and Höhle, 2009; Shean and others, 2016), as an estimate of the maximum potential bias within each elevation bin. That value is 0.49 m. Within each bin, uncertainty about how well the sampled population represents the mean elevation change of the bin is quantified by the median 0.68 quantile of the typically non-gaussian population of elevation differences measured within that bin (Johnson and others, 2013; Larsen and others, 2015). We again made the worst case assumption that errors within each bin are completely correlated. The range of the 0.68 quantile varies from 0.68–7.2 m. The total

uncertainty within a given bin is then the 0.68 quantile expanded by the bias estimate (±0.49 m) on either side.

For comparison with our approach to the extrapolation uncertainty described above, we applied a version of the "simu-laser" approach (Berthier and others 2010). Previous applications of this technique to the UAF LiDAR data concluded that centerline profiles are representative of elevation changes across the entire bin (Johnson and others, 2013; Das and others, 2014). We assessed the representativeness of the 2007 profiles at Eklutna Glacier in the same way, by resampling the full coverage 2010 and 2014 datasets on the profile postings, differencing them, and comparing the calculated uncertainty estimate to our best estimate of the true difference using all available data. We found that, within each bin, our best estimate of the 2010–2014 DEM difference using full DEM coverage was within the range of the uncertainties for the resampled 2010–2014 difference based on the 2007 profile locations and 2007–2010 uncertainty methods. Additionally, the uncertainties for the resampled 2010–2014 difference based on the 2007 profile locations were generally larger than the uncertainties based on the full DEM difference (Supplement S5).

S3.2. 2010–2011, 2010–2012

The 2010, 2011, and 2012 LiDAR data sets all have nominal absolute errors of 0.3 m. Compared to the 2007–2010 interval, the 2010–2011 and 2010–2012 intervals had more overlapping off-glacier data, allowing us to estimate any bias in the original co-registration to the 2010 data by directly co-registering the 2011 and 2012 swaths to each other. The observed xyz shift, between 2011 and 2012, of 0.15 m was then added to the 0.68 quantile (range of variance 0.32–5.3 m) within each bin as we did to the 2007–2010 estimates.

S3.3. 2010–2014

The nearly full coverage of the 2014 DEM allowed us to assess bin-wide uncertainties through an assessment of spatial auto-correlation as we previously did with the 2015 DEM. The resulting range of the total uncertainty within a given bin is 0.30–1.18

S4 **Results**

Raw surface elevation changes and the partitioned elevation changes to make those measurements comparable with the mass balance measurements are shown in Fig. S2 for each of the additional time periods. Annual results for all of the data (2007–2015) are shown for the firn model, late season ablation estimates, and flux divergence rates in Figs. S3, S4, and S5. The ice fluxes for each period are shown in Fig. S6.

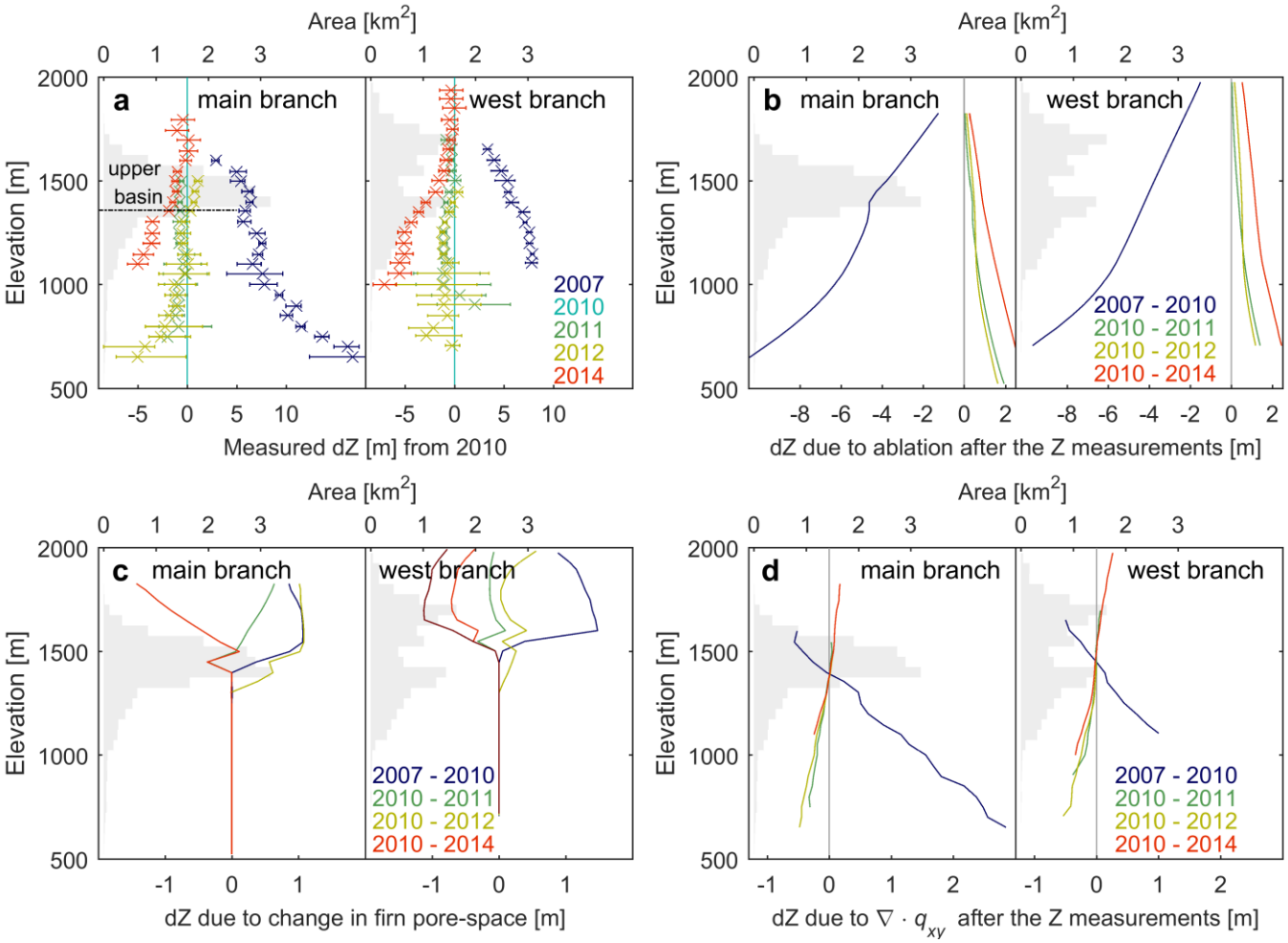

Fig. S2 Measured and calculated changes in surface elevation, by 50 m elevation bin, for the main and west branches of Eklutna Glacier. All panels show the 2010 glacier surface hypsometry in gray with values on the upper horizontal axis. a) Mean (or median in the case of swath and profile data) differences of raw surface elevation measurements, for the years 2007, 2011, 2012, and 2014, from the measured 2010 surface. These are derived from measurements shown in figure 4. Error bars reflect measurement uncertainty. b) Elevation changes, for each interval, caused by ablation that occurred between the surface elevation measurement date and fall mass balance measurement date at beginning and end of the interval. c) Elevation changes due to changes in firn density profiles during the interval. d) Elevation changes due to ice flow (from flux divergence rates) between the surface elevation and mass balance measurement dates.

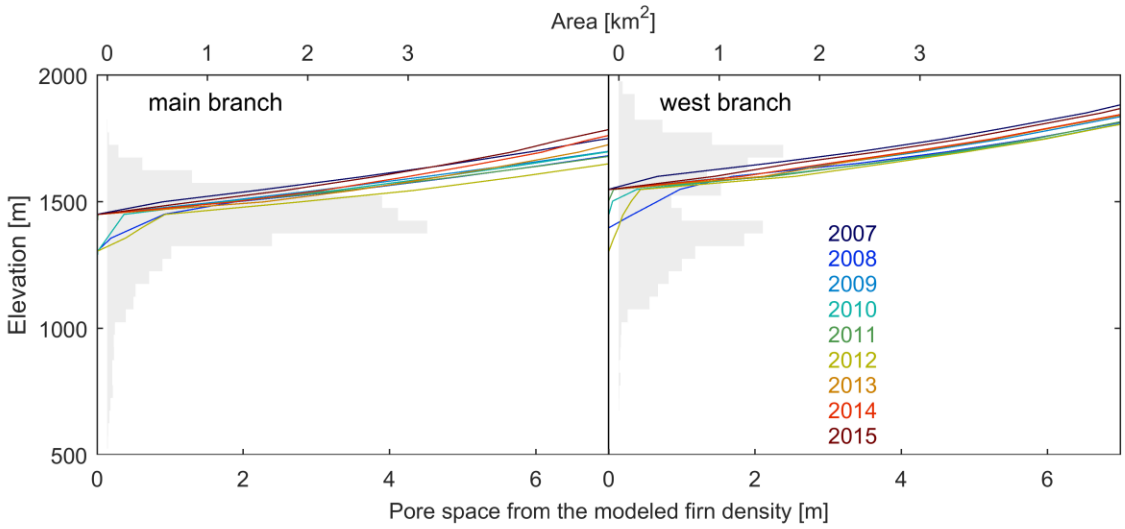

Fig. S3 Firn model results, expressed as the total pore space expressed in m per unit area (i.e. m^3 m^{-2}; to allow direct comparison to the surface elevation change and mass balance rates).

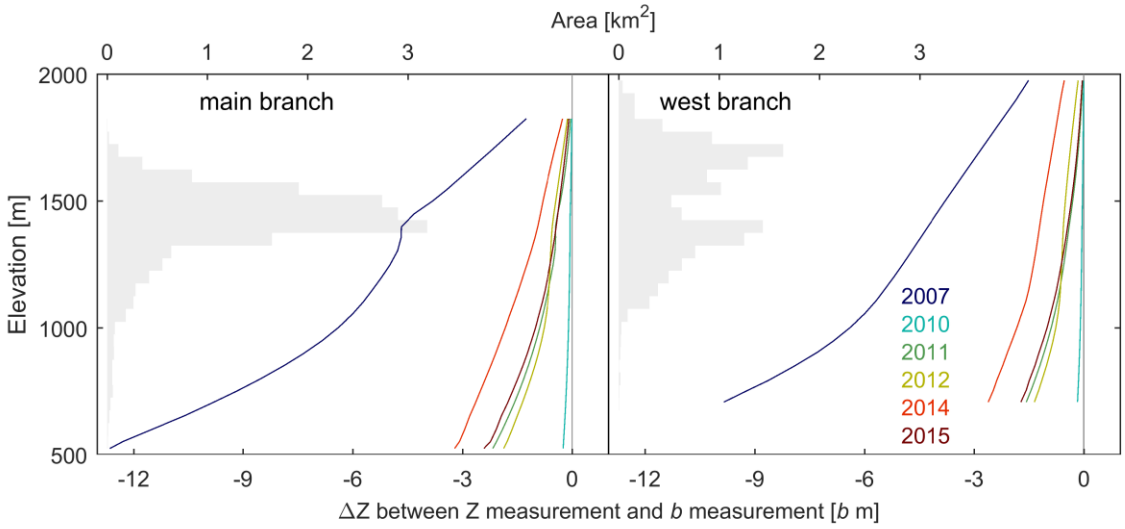

Fig. S4 Late season ablation, expressed as m.

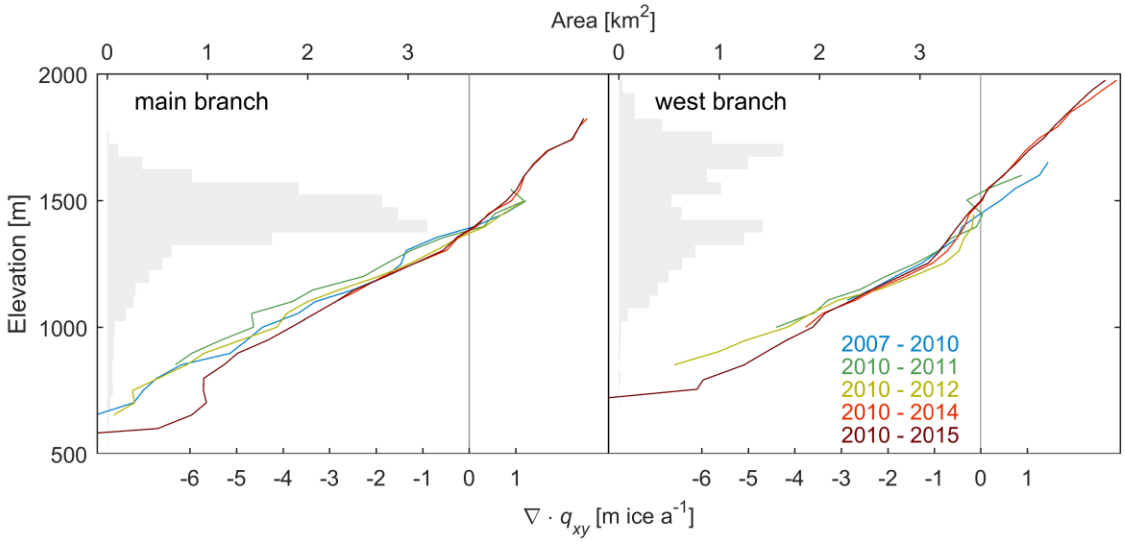

Fig. S5 Summer flux divergence rates, meters per year.

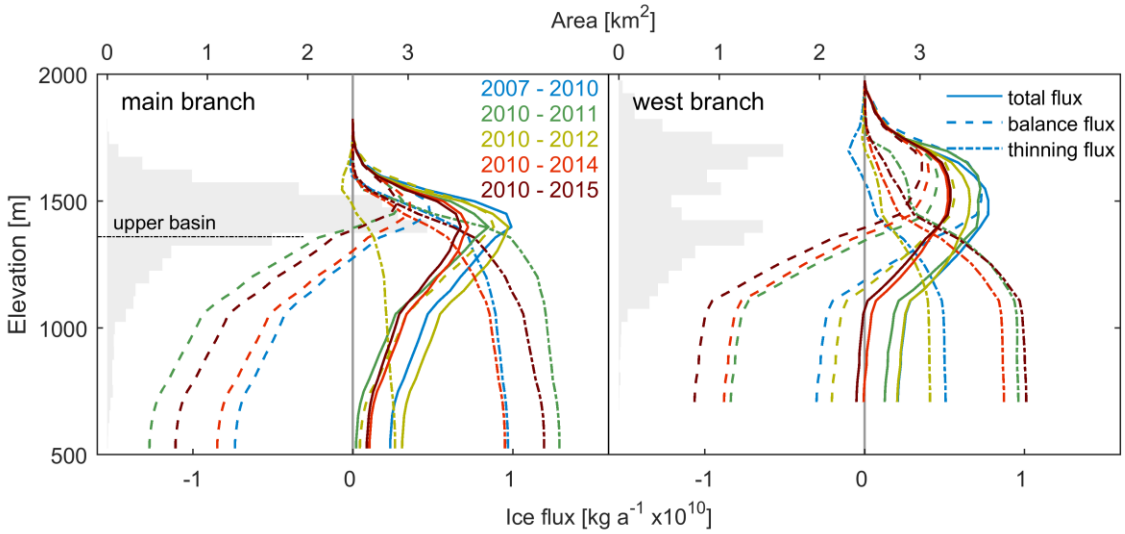

Fig. S6 The balance, thinning, and total ice fluxes 2007–2010, 2010–2011, 2010–2012, and 2010–2014.

S5 **Geodetic check**

The geodetic check requires glacier-wide estimates of thinning rates, but in 2007 there were some areas above the highest elevation measurements, and the 2014 DEM does not cover the terminus. To estimate thinning rates for these unmeasured elevations we assumed the flux divergence was steady over the study period, and used the balance profiles and Equation (2) to estimate the volume change. This assumption introduces some error. Over the various time periods between 2007 and 2014, the maximum range of flux divergence rates at a given elevation was 1.8 m (Fig. S5), so we assigned an uncertainty of ±2.0 m for the areas and time periods with unmeasured surface elevation changes. The geodetic mass balance was then calculated from the total volume change, assuming a density of 900 kg/m^2 for ice and directly accounting for the change in density structure above the ELA with the firn model results.

Table S1. Comparison of the mean glaciological and geodetic mass balances (m w.e. a^{-1}) for 2007–2010 and 2010–2014.

Period	Branch	Glaciological mass balance	Geodetic mass balance
2007–2010	Main branch	−0.42	−0.59 ± 0.60
2007–2010	West branch	−0.22	−0.38 ± 0.82
2007–2010	Glacier-wide	−0.33	−0.50 ± 0.70
2010–2014	Main branch	−0.52	−0.57 ± 0.43
2010–2014	West branch	−0.67	−0.65 ± 0.48
2010–2014	Glacier-wide	−0.59	−0.60 ± 0.45

Table S2. Sensitivity test, showing the change in the error between glaciological and geodetic mass balances in m w.e. after shifting the 2008 and the 2014 mass balance inputs ±1 m w.e.

Period	Branch	Shift glaciological input	Change in Glaciological/Geodetic error
2007–2010	Main branch	+1.0, −1.0	−0.87, +0.90
2007–2010	West branch	+1.0, −1.0	−0.69, +0.99
2007–2010	Glacier-wide	+1.0, −1.0	−0.78, + 0.96
2010–2014	Main branch	+1.0, −1.0	−1.24, +0.88
2010–2014	West branch	+1.0, −1.0	−0.36, +1.16
2010–2014	Glacier-wide	+1.0, −1.0	−0.92, +1.04

Table S3. Velocity measurements from Eklutna Glacier. UTM coordinates of each site accompany a general description of location on glacier. Rows in bold are used to calculate average summer velocities. Year-round velocities are averages, weighted by duration of observation, of all available measurements. Abbreviations and units: d = displacement in meters, v = velocity in meters per year, and 2σ = 95% confidence interval in meters per year.

6784631N, 394371E (upper main branch)					6787853N, 394859E (mid main branch)					6789554N, 394198E (low main branch)				
date 1	date 2	d	v	2σ	date 1	date 2	d	v	2σ	date 1	date 2	d	v	2σ
										02/22/09	05/14/09	8.51	38.3	1.3
05/08/09	**09/12/09**	**2.99**	**8.6**	**0.8**	**05/10/09**	**09/12/09**	**8.75**	**25.6**	**0.8**					
09/12/09	05/26/10	6.50	9.3	0.9	09/12/09	05/22/10		23.6	0.9					
05/26/10	**09/22/10**	**2.85**	**8.8**	**0.9**	**05/22/10**	**09/22/10**	**7.70**	**22.9**	**0.8**	**05/22/10**	**09/22/10**	**14.39**	**42.8**	**1.3**
09/22/10	05/12/11	6.32	9.9	0.4	09/22/10	05/12/11	14.37	22.6	0.4	09/22/10	05/14/11	22.88	35.7	0.4
05/12/11	**09/18/11**	**3.07**	**8.7**	**0.8**	**05/12/11**	**09/18/11**	**7.93**	**22.5**	**0.8**	**05/14/11**	**09/18/11**	**14.47**	**41.5**	**0.8**
					09/18/11	05/14/12	14.36	21.9	0.4	09/18/11	01/18/12	11.58	34.7	0.8
05/15/12	**09/09/12**	**3.48**	**10.9**	**0.9**	**05/14/12**	**09/09/12**	**8.14**	**25.3**	**0.9**					
Average summer velocity			9.2		Average summer velocity			24.1		Average summer velocity			42.2	
Average year-round velocity			9.4		Average year-round velocity			23.2		Average year-round velocity			38.2	

6791626N, 393290E (lower glacier)					6787142N, 391638E (west branch)				
date 1	date 2	d	v	2σ	date 1	date 2	d	v	2σ
05/09/09	**09/11/09**	**21.42**	**62.4**	**1.3**	**06/09/10**	**09/21/10**	**6.64**	**23.4**	**17.6**
09/11/09	05/24/10	37.07	53.1	2.5	09/21/10	05/14/11	11.03	17.1	0.4
05/24/10	**09/21/10**	**20.14**	**61.2**	**2.5**					
09/21/10	05/14/11	33.58	52.2	0.9	09/18/11	05/17/12	10.93	16.5	0.4
05/14/11	**09/18/11**	**20.72**	**59.5**	**0.8**	**05/17/12**	**09/09/12**	**7.45**	**23.6**	**0.9**
05/16/12	**09/09/12**	**19.40**	**61.3**	**0.9**					
Average summer velocity			61.1		Average summer velocity			23.5	
Average year-round velocity			56.9		Average year-round velocity			18.9	

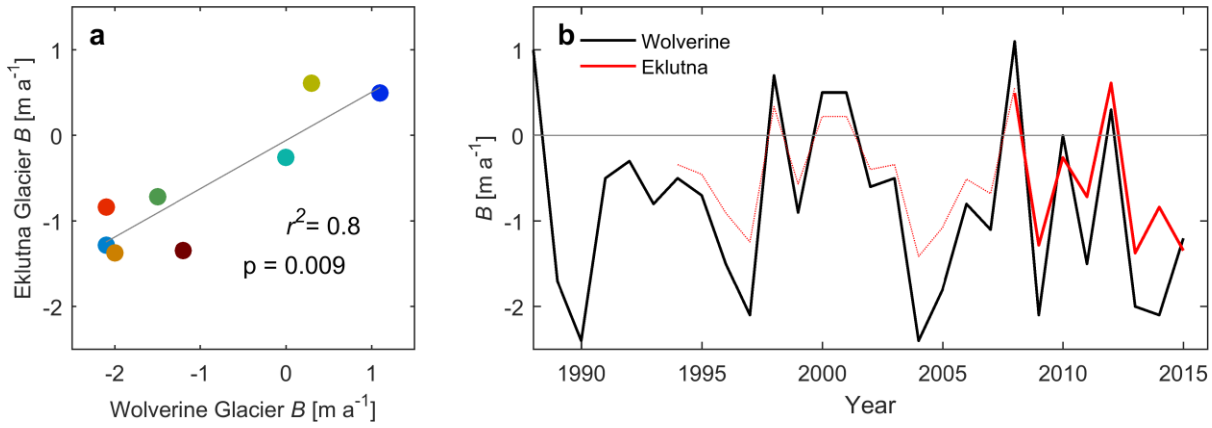

Fig. S7 a) The relationship between Wolverine Glacier and Eklutna Glacier mass balances. Colors correspond to Fig. S3, from blue to red is 2008 to 2015. b) Annual mass balance at Wolverine Glacier from 1988–2015, and at Eklutna Glacier from 2008–2015. The dotted line shows an inferred time series for Eklutna Glacier based on the relationship in 2008–2015.

S6 Results from the "simulaser" analysis

In both branches the median value from the full DEM differences is within the extracted simulaser estimate in all cases (Figure S8). In the main branch 14 of the 18 error bars overlap, with a maximum of 0.23 m between the outside of the full DEM difference based estimate and the outside of the simulaser estimate. In the west branch only 8 of the 18 error bars overlap, and the maximum difference between the outside of the simulaser estimate and the outside of the DEM estimate is 0.37 m.

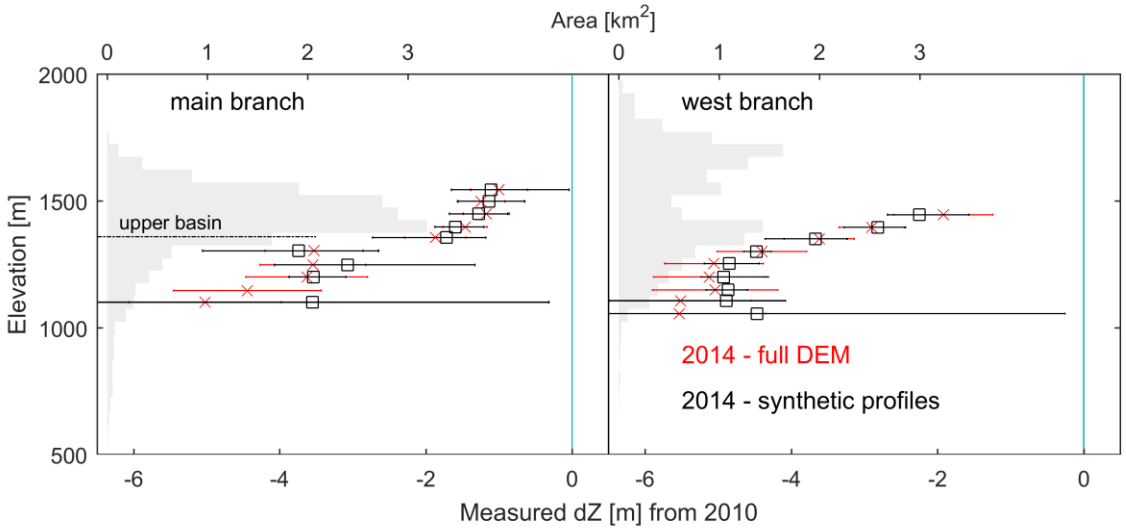

Fig. S8 Comparison of the 2010–2014 full DEM differences (red x's) to the 2010–2014 differences sampled only on the 2007 profile locations. The error bars show the median 68% IQR for the synthetic profiles and the bin uncertainties from equation (9) for the full DEM difference.

S7 **References**

Berthier E, Schiefer E, Clarke GKC, Menounos B and Rémy F (2010) Contribution of Alaskan glaciers to sea-level rise derived from satellite imagery. *Nature Geoscience* **3**(2), 92–95 (doi:10.1038/ngeo737)

Das I, Hock R, Berthier E and Lingle CS (2014) 21st-century increase in glacier mass loss in the Wrangell Mountains, Alaska, USA, from airborne laser altimetry and satellite stereo imagery. *Journal of Glaciology* **60**(220), 283–293 (doi:10.3189/2014JoG13J119)

Echelmeyer K, Harrison W, Larsen C, Sapiano J, Mitchell J, DeMallie J, Rabus B, Adalgeirsdottir G and Sombardier L (1996) Airborne surface profiling of glaciers: A case-study in Alaska. *Journal of Glaciology* **42**(142), 538–547

Höhle J and Höhle M (2009) Accuracy assessment of digital elevation models by means of robust statistical methods. *ISPRS Journal of Photogrammetry and Remote Sensing* 64(4), 398–406

Johnson AJ, Larsen CF, Murphy N, Arendt AA and Zirnheld SL (2013) Mass balance in the Glacier Bay area of Alaska, USA, and British Columbia, Canada, 1995–2011, using airborne laser altimetry. *Journal of Glaciology* **59**(216), 632–648 (doi:10.3189/2013JoG12J101)

Larsen CF (2010) *IceBridge UAF Lidar Profiler L1B geolocated surface elevation triplets, [29 August 2010] Version 1*. NASA Distributed Active Archive Center, National Snow and Ice Data Center, Boulder, CO

Larsen CF, Burgess E, Arendt AA, O'Neel S, Johnson AJ, Kienholz C (2015) Surface melt dominates Alaska glacier mass balance *Geophysical Research Letters* **42**(14) 5209–5908 DOI: 10.1002/2015GL064349

Nuth C and Kääb A (2011) Co-registration and bias corrections of satellite elevation data sets for quantifying glacier thickness change. *The Cryosphere* **5**(1), 271–290

Shean DE, Alexandrov O, Moratto Z, Smith BE, Joughin IR, Porter CC, and Morin PJ, (2016) An automated, open-source pipeline for mass production of digital elevation models (DEMs) from very high-resolution commercial stereo satellite imagery, *ISPRS J. Photogramm. Remote Sens*, 2016 Jun 30 (116) 101–117.